

## **Bimetallic doped carbon dot nanozymes for enhanced sonodynamic and nanocatalytic therapy**

Yandong Huang<sup>a,1</sup>, Lanting Jia<sup>a,1</sup>, Shiqi Zhang<sup>a,1</sup>, Lang Yan<sup>b,\*</sup>, Lei Li<sup>c,\*</sup>

<sup>a</sup> Department of Ultrasound, Second Affiliated Hospital of Naval Medical University, Shanghai 200003, China

<sup>b</sup> Department of Health Toxicology, Faculty of Naval Medicine, Naval Medical University, Shanghai 200433, China

<sup>c</sup> Department of Emergency, Changhai Hospital, Naval Medical University, Shanghai 200433, China

\* Corresponding authors.

*E-mail addresses:* langyan@smmu.edu.cn (L. Yan), relayinch@smmu.edu.cn (L. Li)

<sup>1</sup> These authors contributed equally to this work.

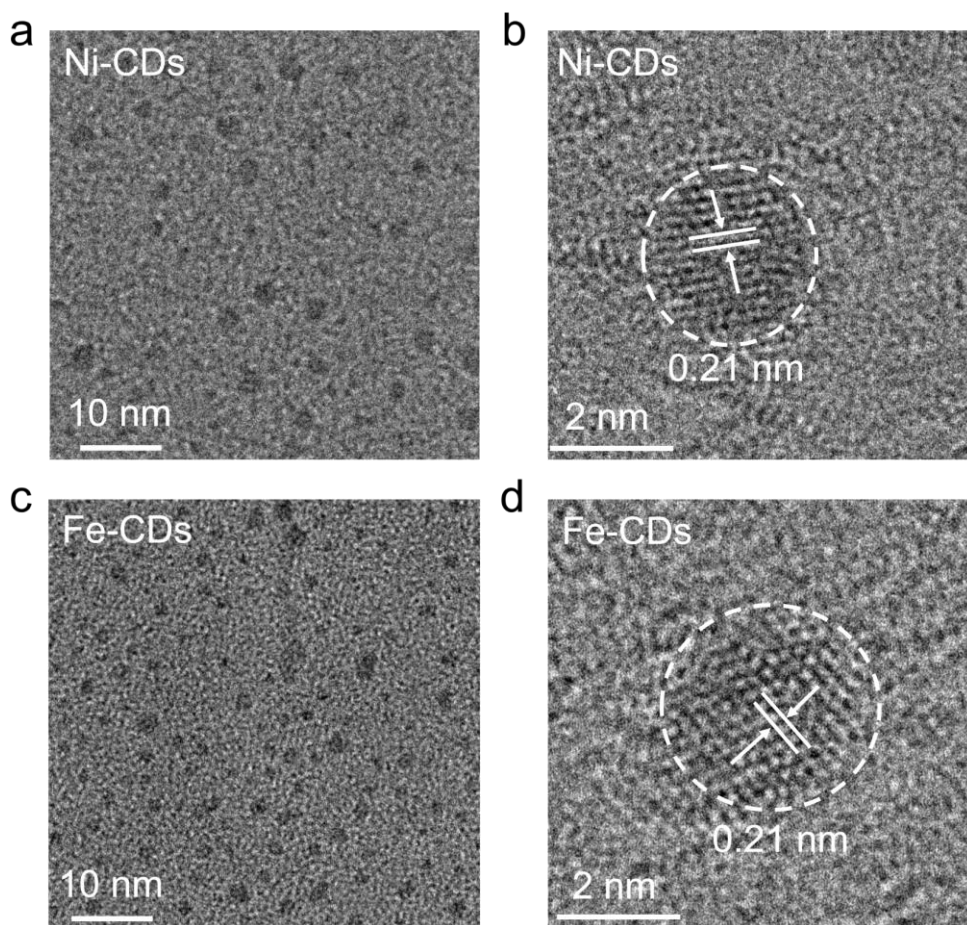


**Fig. S1** TEM and high-resolution TEM images of Ni-CDs and Fe-CDs.

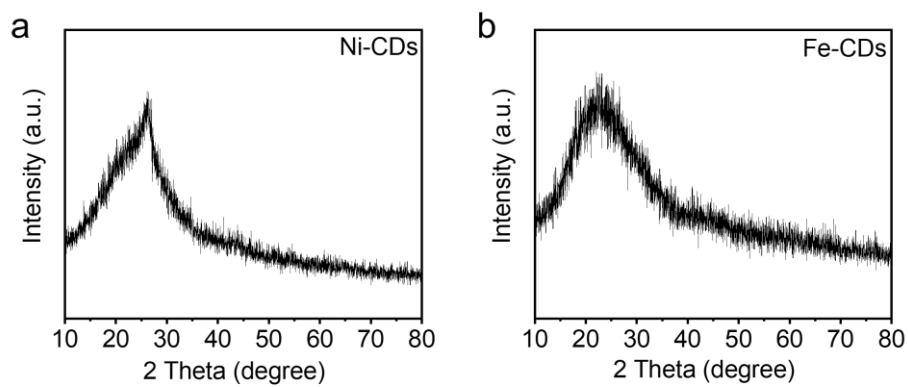


**Fig. S2** XRD patterns of Ni-CDs and Fe-CDs.

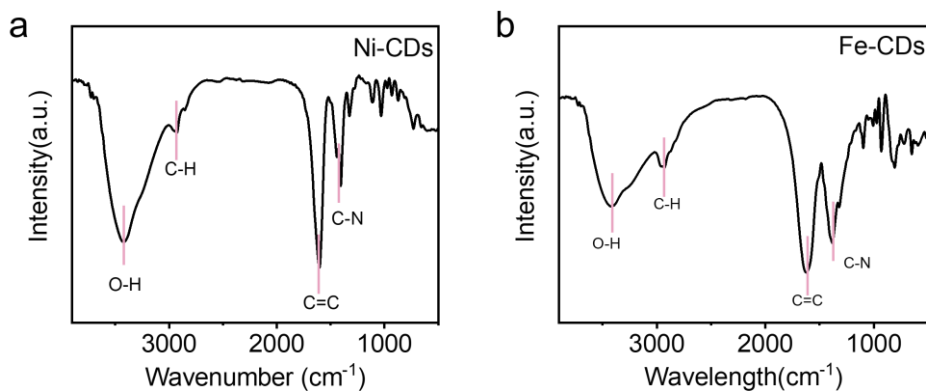


**Fig. S3** FTIR spectra of Ni-CDs and Fe-CDs.

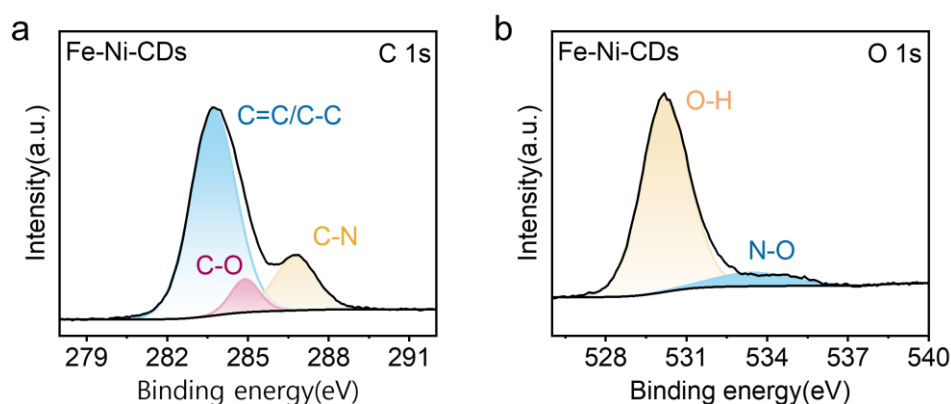


**Fig. S4** High-resolution C 1s and O 1s spectra of Fe-Ni-CDs.

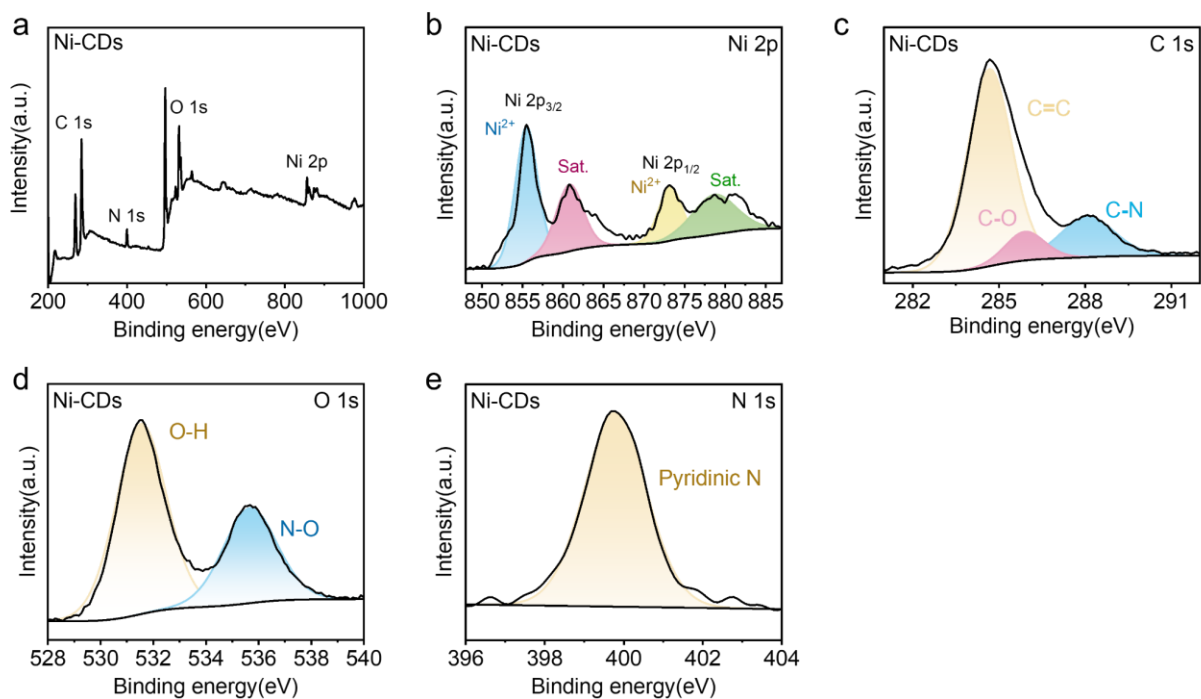


**Fig. S5** The survey XPS, high-resolution Ni 2p, C 1s, O 1s, and N 1s spectra of Ni-CDs.

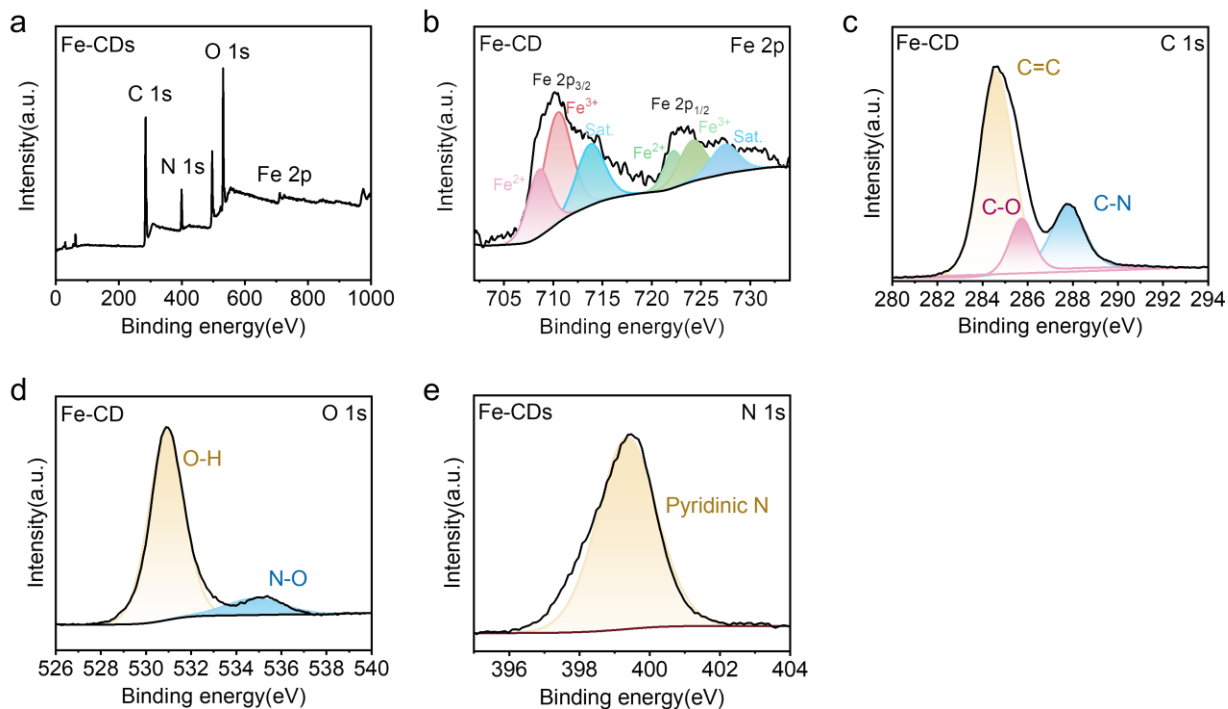


**Fig. S6** The survey XPS, high-resolution Fe 2p, C 1s, O 1s, and N 1s spectra of Fe-CDs.

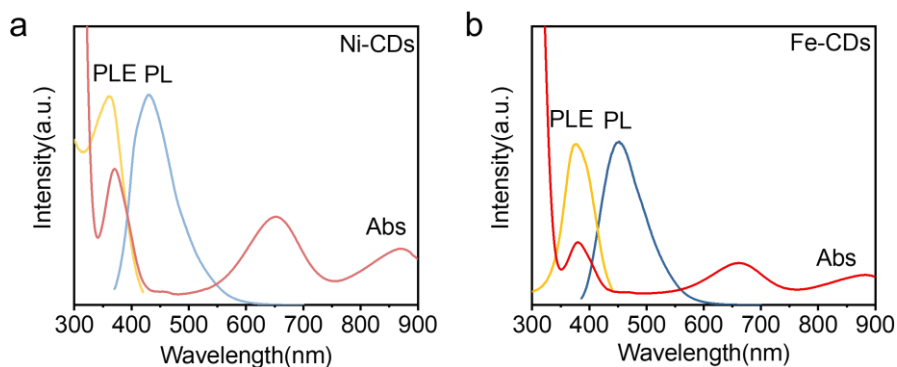


**Fig. S7** Absorption, PL, and PLE spectra of Ni-CDs and Fe-CDs.

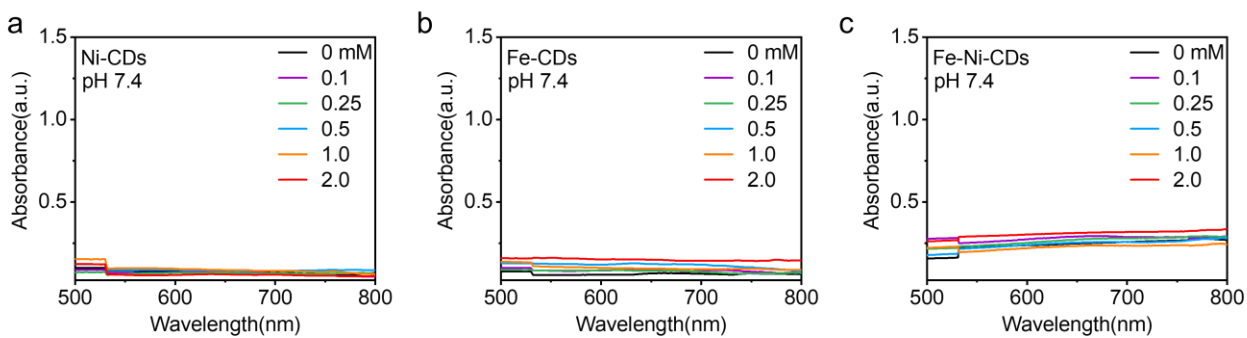


**Fig. S8** Evaluation of POD-mimic catalytic activity of Ni-CDs and Fe-CDs in the presence of  $H_2O_2$  with varied concentrations at pH 7.4.

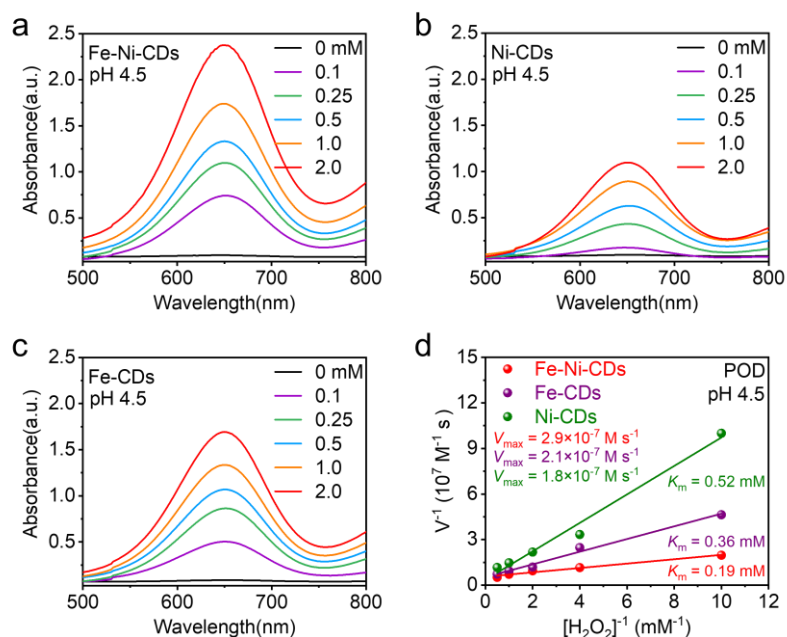


**Fig. S9** (a-c) Evaluation of POD-mimic catalytic activity of Fe-Ni-CDs, Ni-CDs, and Fe-CDs in the presence of  $\text{H}_2\text{O}_2$  with varied concentrations at pH 4.5. (d) Comparison of the POD-mimic catalytic activity of these three kinds of CDs at pH 4.5.

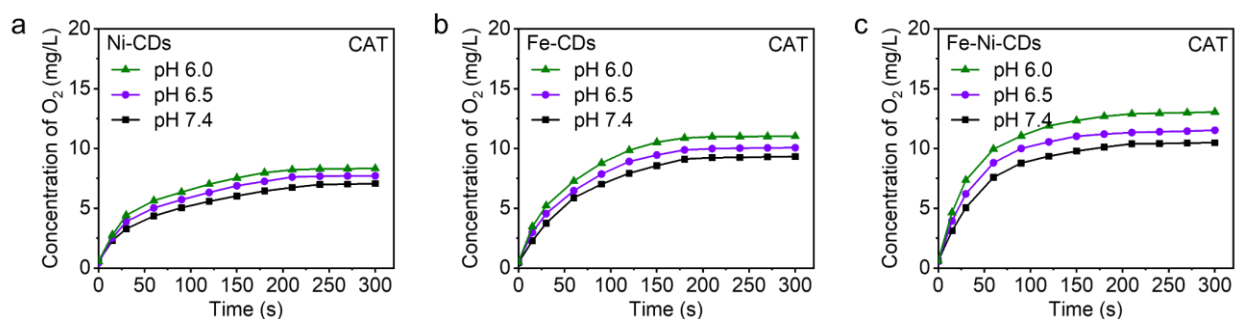


**Fig. S10** Evaluation of CAT-mimic catalytic activity of Ni-CDs, Fe-CDs, Fe-Ni-CDs in the presence of  $\text{H}_2\text{O}_2$  at varied pH.

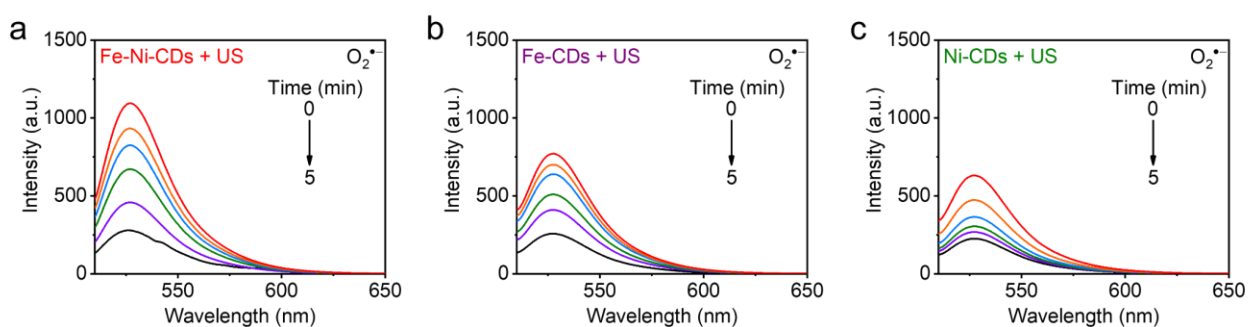


**Fig. S11** (a-c) The fluorescence spectra of DHR123 in the presence of Fe-Ni-CDs (a), Fe-CDs (b), or

Ni-CDs (c) under US irradiation for different times (0-5 min).

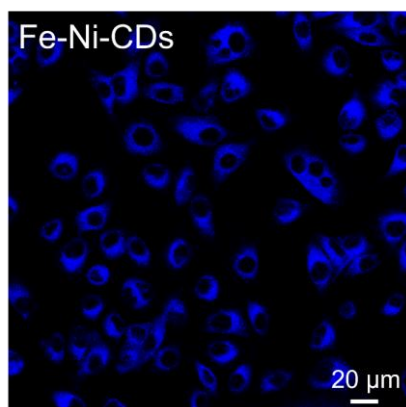


**Fig. S12** Cellular uptake of Fe-Ni-CDs in 143B cells.

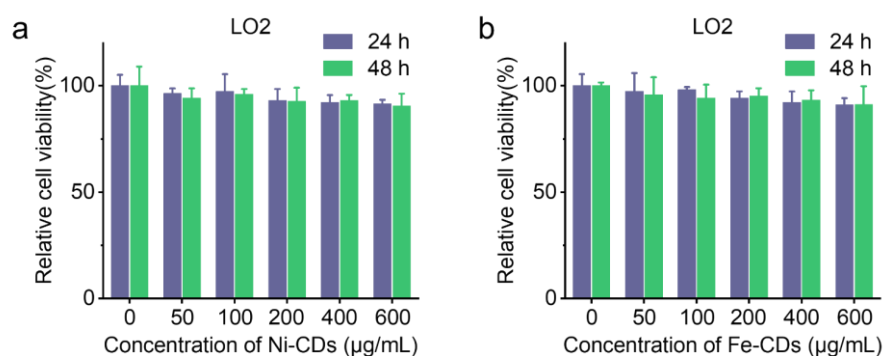


**Fig. S13** (a, b) Relative cell viabilities of LO2 cells incubated with Ni-CDs and Fe-CDs with varied concentrations for 24 or 48 h.

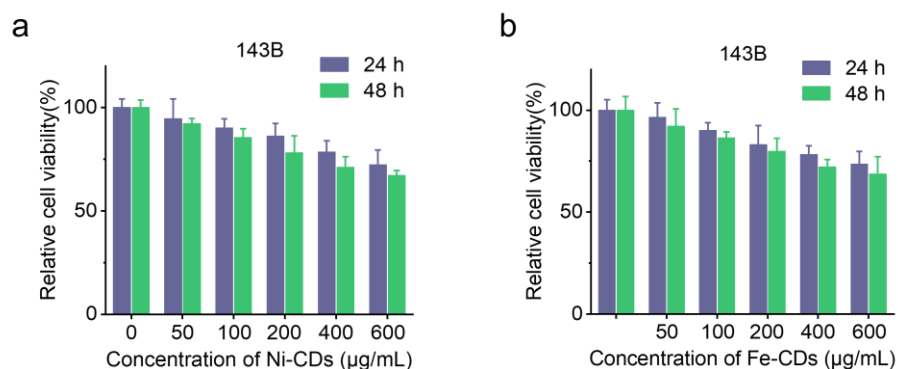


**Fig. S14** (a, b) Relative cell viabilities of 143B cells incubated with Ni-CDs and Fe-CDs with varied concentrations for 24 or 48 h.

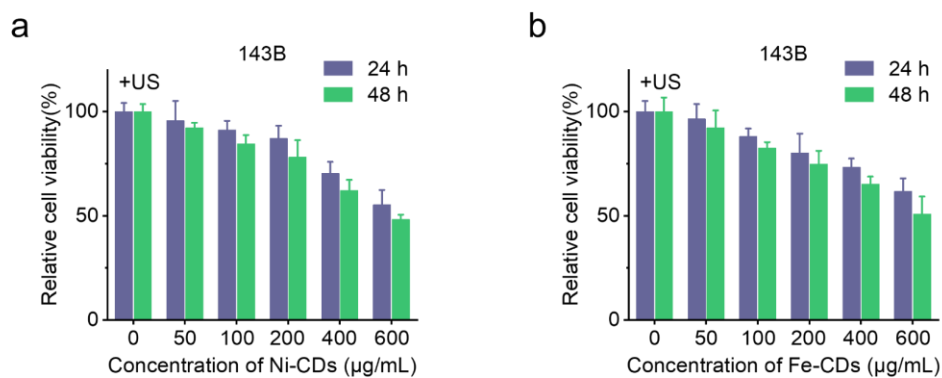


**Fig. S15** (a, b) Relative cell viabilities of 143B cells incubated with Ni-CDs and Fe-CDs with varied concentrations for 24 or 48 h in the presence of US irradiation.

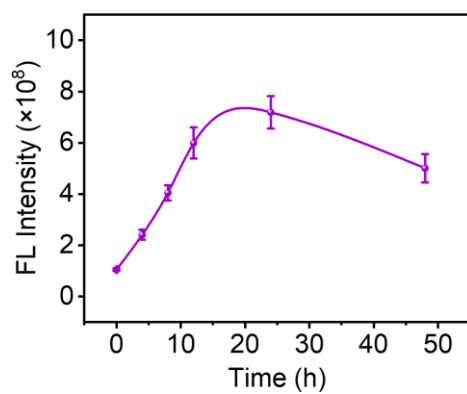


**Fig. S16** The quantitative results of in vivo fluorescence imaging.

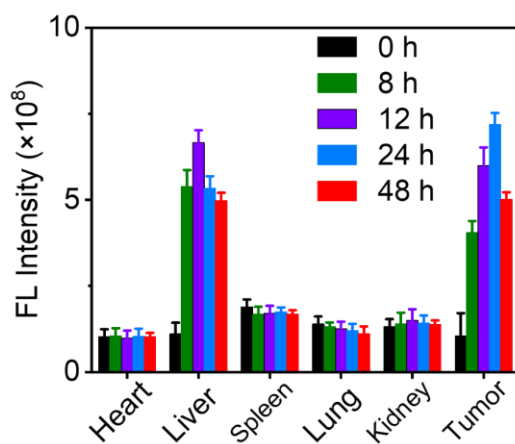


**Fig. S17** Time-dependent fluorescence intensity of Fe-Ni-CDs in the major organs and tumor tissues.

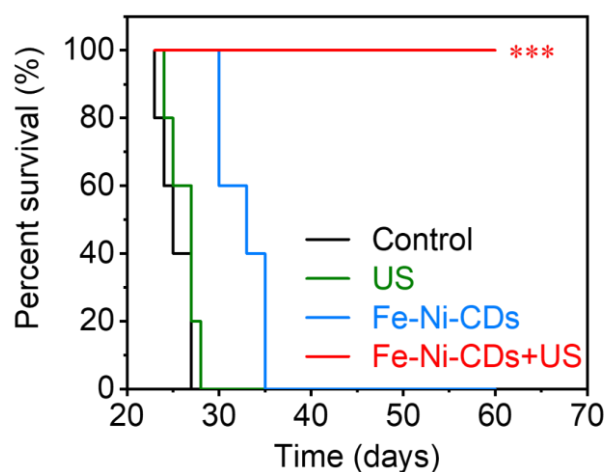


**Fig. S18** Survival rate of mice after different treatments.

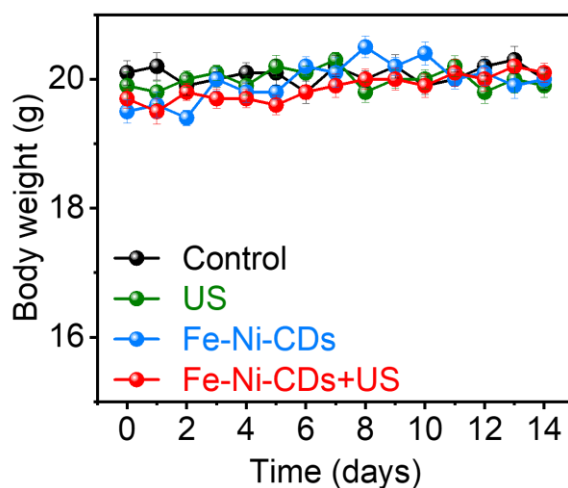


**Fig. S19** Body weight of mice after different treatments.

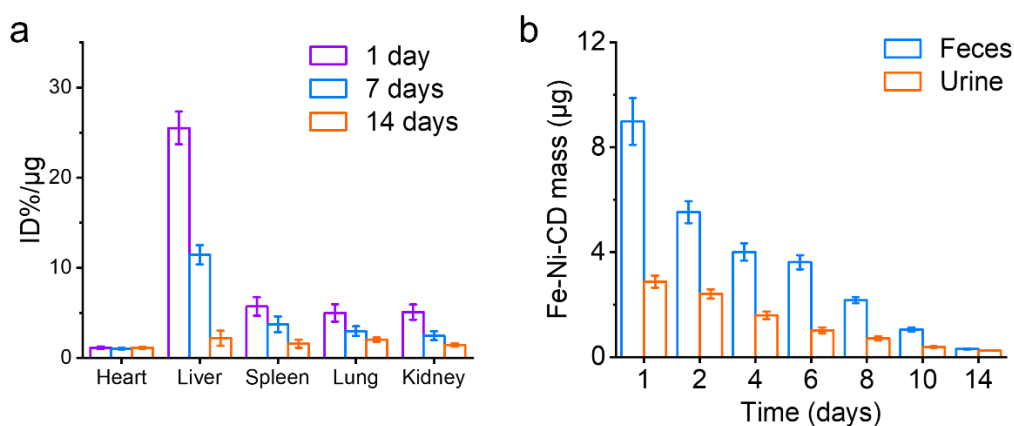


**Fig. S20** (a) Biodistribution of Fe-Ni-CDs post i.v. injection in mice on different days. (b) The detected Fe-Ni-CD mass in urine and feces at different time points post i.v. injection of Fe-Ni-CDs.



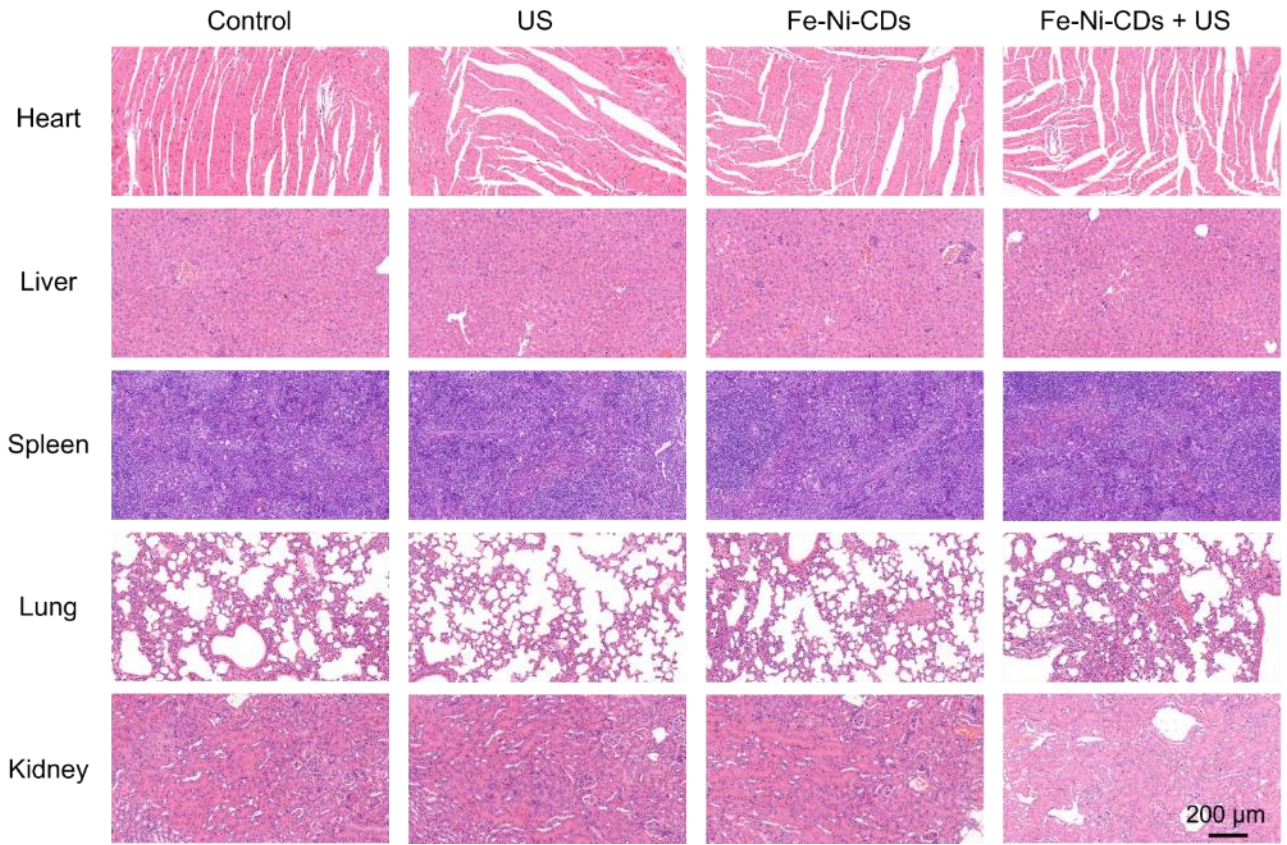


**Fig. S21** H&E-stained images obtained from the major organs (heart, liver, spleen, lung, and kidney) of mice in different treatment groups.

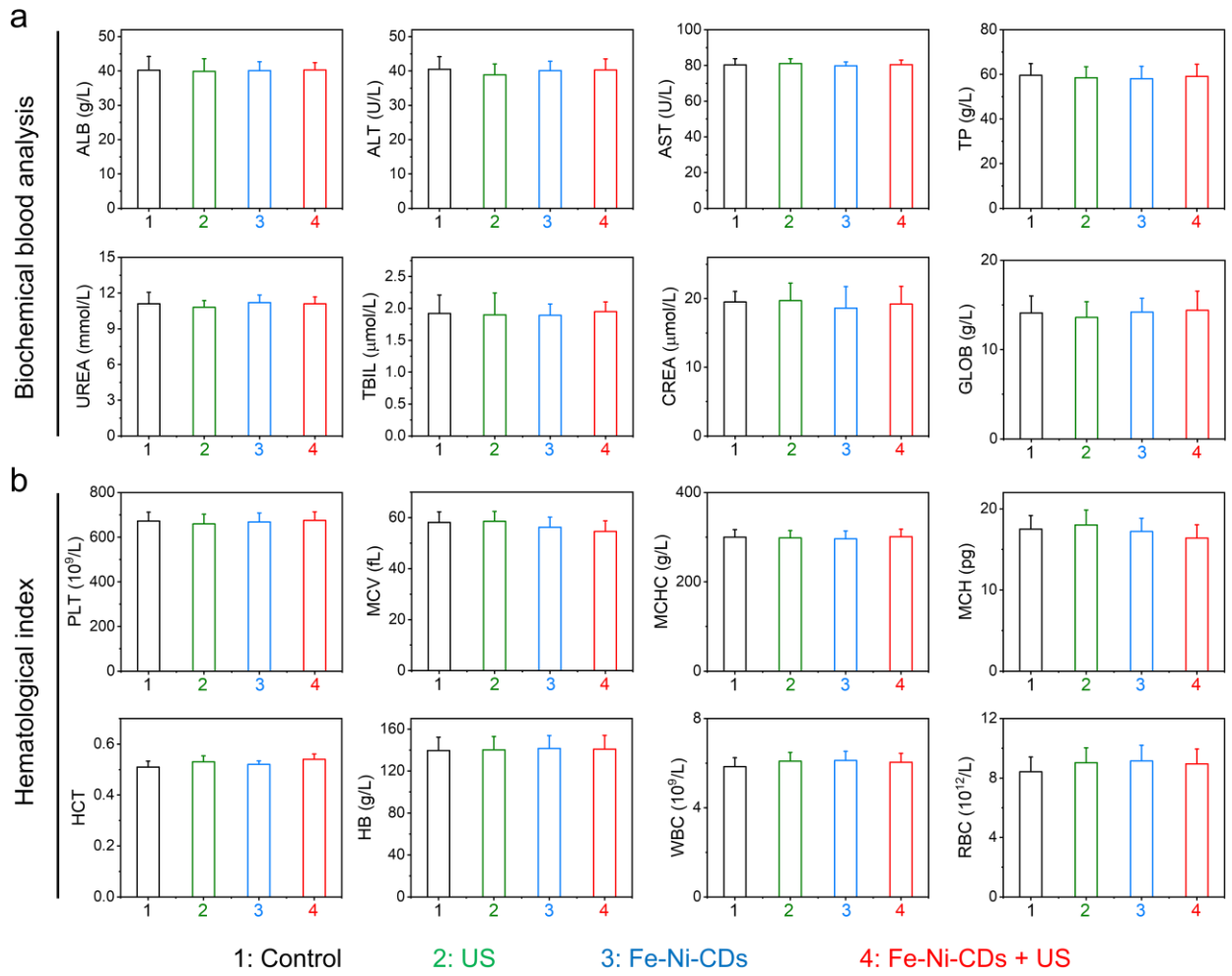


**Fig. S22** (a-b) Biochemical blood analysis (a) and hematological index (b) of the mice that were sacrificed at 18 days after different treatments. The terms of biochemical blood analysis include ALB, ALT, AST, TP, UREA, TBIL, CREA, and GLOB. The terms of hematological index include PLT, MCV, MCHC, MCH, HCT, Hb, WBC, and RBC.

**Table S1.** Comparison of the POD-mimic catalytic activity of Fe-Ni-CDs with previously reported metal-carbon nanozymes.<sup>1-6</sup>

Sample (POD-like enzyme)	$K_m$	$V_{max}$	Ref.
<b>Fe-Ni-CDs</b>	<b>0.26 mM</b>	<b><math>2.90 \times 10^{-7} \text{ M s}^{-1}</math></b>	<b>This work</b>
FeP/CDs	0.84 mM	$1.55 \times 10^{-6} \text{ M s}^{-1}$	1
Fe-CDs	97.64 mM	$4.24 \times 10^{-7} \text{ M s}^{-1}$	2
CDs <sub>EDTA</sub> -Fe	0.079 mM	$8.57 \times 10^{-8} \text{ M s}^{-1}$	3
CDs <sub>EDTA</sub> -Ni	0.07 mM	$1.23 \times 10^{-8} \text{ M s}^{-1}$	3
Pt@CD	26.5 mM	$9.10 \times 10^{-8} \text{ M s}^{-1}$	4
NPCG-900	0.35 mM	$8.66 \times 10^{-8} \text{ M s}^{-1}$	5
N-HCNs@AuNPs	290 mM	$12.9 \times 10^{-8} \text{ M s}^{-1}$	6

**Table S2.** Comparison of the CAT-mimic catalytic activity of Fe-Ni-CDs with previously reported metal-carbon nanozymes.<sup>7,8</sup>

Sample (CAT-like enzyme)	$K_m$	$V_{max}$	Ref.
<b>Fe-Ni-CDs</b>	<b>0.39 mM</b>	<b><math>3.01 \times 10^{-6} \text{ M s}^{-1}</math></b>	<b>This work</b>
Mn-SANs	11.6 mM	$4.53 \times 10^{-5} \text{ M s}^{-1}$	7
Pt@CNDs	42.84 mM	$0.41 \times 10^{-6} \text{ M s}^{-1}$	8

## References

1. J. Dong, G. Liu, Y. V. Petrov, Y. Feng, D. Jia, V. E. Baulin, A. Yu Tsivadze, Y. Zhou, B. Li, *Adv. Healthc. Mater.*, 2024, 2402568.
2. Y. Liu, B. Xu, M. Lu, S. Li, J. Guo, F. Chen, X. Xiong, Z. Yin, H. Liu, D. Zhou, *Bioact. Mater.*, 2022, **12**, 246.
3. J. Dong, G. Liu, Y. V. Petrov, Y. Feng, D. Jia, V. E. Baulin, A. Y. Tsivadze, Y. Zhou, B. Li, *ACS Materials Lett.*, 2024, **6** (4), 1112.
4. C. Liu, J. Hu, W. Yang, J. Shi, Y. Chen, X. Fan, W. Gao, L. Cheng, Q.-Y. Luo, M. Zhang, *Nanoscale*, 2024,

**16** (9), 4637.

5. S. Yi, H. Zhao, X. Xu, B. Guan, H. Zhao, R. Zhang, *Appl. Surf. Sci.*, 2024, **655**, 159568.
6. Z. Wang, Z. Xu, X. Xu, J. Xi, J. Han, L. Fan, R. Guo, *Colloid. Surface. B*, 2022, **217**, 112671.
7. C. S. Wang, H. B. Xue, L. Zhuang, H. P. Sun, H. Zheng, S. Wang, S. He, X. B. Luo, *ACS Omega*, 2023, **8** (51), 49289.
8. Y. Zhang, W. Gao, Y. Ma, L. Cheng, L. Zhang, Q. Liu, J. Chen, Y. Zhao, K. Tu, M. Zhang, C. Liu, *Nano Today*, 2023, **49**, 101768.